

which is known only approximately. Since an error of 0.1 Å in $\bar{R} - 2\xi$ may cause an error in $k(T)$ approaching a factor of 10^4 , it is not feasible to calculate absolute rate constants. By the same token, it is not possible to fix \bar{J} accurately in our present calculations where $k(T)$ is used as an input parameter: the values of \bar{J} used in the examples thus show wide variations. Nevertheless, these \bar{J} values may still provide a useful indication of the absolute accuracy of $\bar{R} - 2\xi$. On physical grounds one expects \bar{J} to increase sharply (rough exponentially) with decreasing $\bar{R} - 2\xi$. However, in our applications, small distances often lead to small couplings. This probably means that $\bar{R} - 2\xi$ has been underestimated in these cases and that the resulting error is compensated by a low value of \bar{J} .

These considerations suggest a specific approach to improve the model. The coupling \bar{J} can in principle be removed as an adjustable parameter, since $J_{AB}(R)$ is amenable to quantum-chemical calculation. In several of the examples presented, this would undoubtedly give rise to a substantial change of the other parameters and probably a poorer reproduction of the experimental data. This in turn would indicate the need for a more accurate

description of the reaction path, specifically for the inclusion of an XH-bending along with an XH-stretching coordinate. Such improvements will be considered in forthcoming publications.

The examples treated here show, however, that the model in its simple form is adequate for a semiquantitative interpretation of hydrogen-tunneling reactions, especially in systems approaching collinearity. It gives a much more realistic picture of the transfer than the conventional tunneling approach and may permit one to draw specific conclusions about the mechanism of the transfer. Its assignment of numbers to specific molecular properties suggests new experiments and new calculations, which, we hope, will stimulate research in this area.

Acknowledgment. We are grateful to Keith Ingold for his comments and encouragement.

Registry No. 2,4,6-Tri-*tert*-butylphenyl, 53054-78-7; 2-methylacetophenone *cis*-enol, 85562-08-9; *trans*-2,3,4,4a,9,9a-hexahydro-4a,9-dimethylindole, 20890-47-5; dimethylglyoxime, 95-45-4; *trans*-4a,4b-dihydrophenanthrene, 33431-13-9; methyl, 2229-07-4; *meso*-tetraphenylphosphine, 917-23-7.

Monte Carlo Studies of a Dilute Aqueous Solution of Benzene

P. Linse,*† G. Karlström,† and B. Jönsson†

Contribution from Physical Chemistry 1 and 2, Chemical Center, University of Lund, S-220 07 Lund, Sweden. Received September 21, 1983

Abstract: A dilute aqueous solution of benzene has been examined by Monte Carlo simulations using pairwise additive potentials obtained from ab initio quantum chemical calculations. The water molecules in the first hydration shell around a benzene molecule show a preferential orientation according to the electrostatic dipole-quadrupole interaction. However, the water-water distribution functions for molecules close to the benzene molecule show only small deviations from what is found in pure water. The two models studied, periodic, boundary conditions and the cluster model, have a stronger influence on the properties calculated than the presence of a benzene molecule.

Dilute aqueous solutions are of fundamental importance, and in recent years, computer simulation methods such as Monte Carlo (MC) and molecular dynamic (MD) techniques have provided detailed molecular information on the structure of water around a solute molecule. Such structural and dynamic information is usually very difficult to extract from experiments on dilute solutions. Most computer simulations of aqueous solutions have so far been concerned with small, often spherical, solutes. The solute-water interaction has been described by both empirical¹⁻⁴ and quantum mechanical potentials.⁵⁻¹⁰ Examples of hydrophobic solutes investigated are methane^{5,6} and argon,⁷ but polar nonionic solutes such as methanol,⁸ ethanol,⁹ and formaldehyde¹⁰ have also been considered. In some cases, the solvation effects on the intramolecular structure have been studied explicitly—examples are methanol,⁸ butane,¹¹ and hydrogen peroxide.¹² Computer simulations have also been performed on electrolyte solutions¹³⁻¹⁸ and on solvation of fragments of biomolecules.^{19,20}

A common goal of these simulations has been to study how the solute molecule influences the solvent structure. The generally accepted picture of hydrophobic hydration, arising both from experiment and computer simulations, is that the loose network of hydrogen bonds is strengthened around the nonpolar solute, giving a more ordered water structure.^{21,22} On the other hand, the interaction between an ion and water is quite different. The prevalent picture of ions in aqueous solutions stems from the work of Gurney²³ and Frank and Wen.²⁴ In this case, the orientation

of water molecules close to the ion is governed by the ion-water interaction, and the network of hydrogen bonds is partially destroyed.

- (1) Geiger, A.; Rahman, A.; Stillinger, F. H. *J. Chem. Phys.* **1979**, *70*, 263.
- (2) Okazaki, S.; Nakanishi, K.; Touhara, H.; Adachi, Y. *J. Chem. Phys.* **1979**, *71*, 2421.
- (3) Okazaki, S.; Nakanishi, K.; Touhara, H.; Watanabe, N.; Adachi, Y. *J. Chem. Phys.* **1981**, *74*, 5863.
- (4) Pangali, C.; Rao, M.; Berne, B. J. *J. Chem. Phys.* **1979**, *71*, 2975, 2982.
- (5) Swaminathan, S.; Harrison, S. W.; Beveridge, D. L. *J. Am. Chem. Soc.* **1978**, *100*, 5705.
- (6) Owicki, J. C.; Scheraga, H. A. *J. Am. Chem. Soc.* **1977**, *99*, 7413.
- (7) Alagona, G.; Tanl, A. *J. Chem. Phys.* **1980**, *72*, 580.
- (8) Bolis, G.; Corongiu, G.; Clementi, E. *Chem. Phys. Lett.* **1982**, *86*, 299.
- (9) Alagona, G.; Tanl, A. *Chem. Phys. Lett.* **1982**, *87*, 337.
- (10) Mehrotra, P. K.; Beveridge, D. L. *J. Phys. Chem.* **1980**, *102*, 4287.
- (11) Jorgensen, W. L. *J. Chem. Phys.* **1982**, *77*, 5757.
- (12) Jönsson, B.; Romano, S.; Karlström, G. *Int. J. Quantum Chem.* **1984**, *25*, 503.
- (13) Briant, C. L.; Burton, J. J. *J. Chem. Phys.* **1976**, *64*, 2888.
- (14) Rao, M.; Berne, B. J. *J. Chem. Phys.* **1981**, *85*, 1498.
- (15) Geiger, A. *Ber. Bunsenges. Phys. Chem.* **1981**, *85*, 52.
- (16) Mazei, M.; Beveridge, D. L. *J. Chem. Phys.* **1981**, *74*, 6902.
- (17) Engström, S.; Jönsson, B.; Jönsson, B. *J. Magn. Reson.* **1982**, *50*, 1.
- (18) Lee, W. K.; Prohofsky, E. W. *J. Chem. Phys.* **1981**, *75*, 3040.
- (19) Clementi, E.; Corongiu, G. *Biopolymers* **1981**, *20*, 551.
- (20) Karplus, M.; McCammon, J. A. *CRC Crit. Rev. Biochem.* **1981**, *9*, 293.
- (21) Franks, F. In "Water—A Comprehensive Treatise"; Franks, F. Ed.; Plenum Press: New York, 1972; Vol 2.
- (22) Ben-Naim, A. "Water and Aqueous Solutions"; Plenum Press: New York, 1974.
- (23) Gurney, R. W. "Ionic Processes in Solutions"; McGraw-Hill: New York, 1953.
- (24) Frank, H. S.; Wen, W. Y. *Discuss. Faraday Soc.* **1957**, *24*, 133.

*Physical Chemistry 1.

†Physical Chemistry 2.

Table I. Coefficients of the Fitted Benzene–Water Pair Potential, kJ/mol and Å^a

atom pair, <i>i</i>	<i>A_i</i>	<i>B_i</i>	<i>C_i</i>	<i>D_i</i>	<i>E_i</i>
C–O	1.4089 × 10 ²	6.8602 × 10 ²	−1.0829 × 10 ⁴	1.8788 × 10 ⁵	4.6020 × 10 ⁵
C–H	−7.0445 × 10 ¹	−3.9506 × 10 ²	3.5950 × 10 ³	−2.7238 × 10 ⁴	1.1586 × 10 ⁵
H–O	−1.4089 × 10 ²	−7.3743 × 10 ²	4.7904 × 10 ³	−2.4449 × 10 ⁴	5.8333 × 10 ⁴
H–H	7.0445 × 10 ¹	4.2076 × 10 ²	−2.6898 × 10 ³	9.3717 × 10 ³	1.3059 × 10 ⁴

^aThe molecular geometries used were $r_{CC} = 1.395$ Å, $r_{CH} = 1.084$ Å, $r_{OH} = 0.9572$ Å, and $\Delta HOH = 104.52$.

In this paper, we report MC simulations of a dilute aqueous solution of benzene under canonical ensemble conditions. All simulations are based on pairwise additive potential function representative of ab initio quantum mechanical calculations of the intermolecular interaction.

The purpose of this work is 2-fold. First, in order to understand how the nature of the hydrophobic hydration changes when going from a small inert solute molecule to large surfaces, it is of great value to know how hydrocarbons of different sizes behave in water and how the hydrophobic hydration is affected by the presence of polarizable double bonds as in benzene. Although water and benzene are immiscible at room temperature, the interaction between a water and a benzene molecule is by no means negligible, amounting to −8 to −12 kJ/mol over a large part of the energy hypersurface.²⁵ This can be contrasted with an energy minima of −0.36 kJ/mol for the water–argon⁷ and −2.1 kJ/mol for the water–methane⁶ interactions.

In both MC and MD simulations, some sort of boundary conditions^{26,27} have to be introduced. The boundary conditions may have an unphysical influence on the results, and thus the second purpose of this work is to examine how different boundary conditions affect the structural and energetical results. We have considered two cases, the cluster model and periodic boundary conditions with a cubic cutoff.

Intermolecular Potential Function

The benzene–water intermolecular energy function used in this work has been described by Karlström et al.²⁵ It was obtained from ab initio quantum chemical calculations using the Hartree–Fock self-consistent-field (HF–SCF) approximation, and the dispersion energy contribution was obtained by a perturbation procedure. The resulting intermolecular energy function is a linear combination of atom–atom terms of the form

$$E = \sum_i \left[A_i \frac{1}{r_i} + B_i \frac{1}{r_i^4} + C_i \frac{1}{r_i^6} + D_i \frac{1}{r_i^9} + E_i \frac{1}{r_i^{12}} \right] \quad (1)$$

where *i* sums over the interatomic distances C–O, C–H, H–O and H–H. Table I shows the coefficients for the best fit with a mean-square deviation of 1.0 kJ/mol. Two potential energy curves are shown in Figure 1 demonstrating preferential water orientations depending on whether the water molecule approaches perpendicular to (a) or in (b) the benzene plane, respectively. In the global minimum which is very similar to the minimum structure shown in Figure 1a, the water molecule is tilted slightly away from the benzene symmetry axis. The interaction energy for this geometry is −12.5 kJ/mol from the potential function and −13.2 kJ/mol from the ab initio calculations, respectively.

The water–water interaction energy was evaluated by using the function of Matsuoka et al.,²⁸ based on fairly large ab initio calculations and which is often referred to in the literature.^{5–10,12,15–17,19}

Details of Calculations

General principles of the Monte Carlo method have been reviewed by several authors^{26,29,30} and will not be repeated here. Our

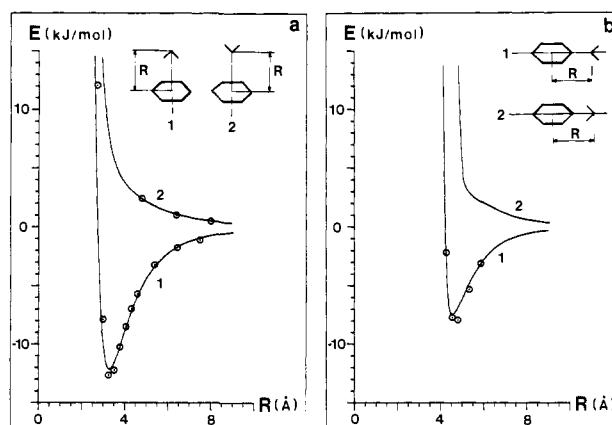


Figure 1. Potential energy curves of benzene and water along two directions with fixed orientations. In 1a, the symmetry axes of the molecules coincide, and in 1b, both molecules are in the same plane. The orientations are shown in the inserts. The circles are ab initio calculated energies, and the lines are fitted energy curves.

Table II. Data about the Simulations

simulation	boundary condition	solvated benzene molecule	cluster radius or box lengths, Å	no. of configur ^d
1w	CM ^a	no	10.86	8 × 10 ⁵
1u	CM ^a	yes	10.96	2 × 10 ⁶
2w	PBC ^b	no	18.84, 18.84, 16.84	2 × 10 ⁶
2b	PBC ^b	yes	18.99, 18.99, 16.99	2 × 10 ⁶
2b' ^c	PBC ^b	yes	18.99, 18.99, 16.99	2 × 10 ⁶

^aCluster model. ^bPeriodical boundary conditions. ^cModified water–benzene potential, see text. ^dEquilibration runs were performed with (1–2) × 10⁶ configurations.

MC calculations have been performed in the canonical (*N*, *T*, *V*) ensemble at a system temperature of 298 K. The algorithm of Metropolis et al.³¹ was modified by using a preferential sampling with a weight function $1/r^2$,^{32,33} with *r* being the distance from the center of mass of the benzene molecule. Thus, water molecules close to the benzene molecule were selected with a higher frequency than those further away. This was done since we are primarily interested in the properties of the solution close to the solute.

Five different simulations have been performed—two of pure water, denoted w, and three simulations including a benzene molecule, denoted b. Two different boundary conditions have been used—the cluster model, denoted 1, and periodic boundary conditions with a cubic cutoff, denoted 2 (see Table II). In the cluster model, all oxygen atoms of the water molecules were constrained

(25) Karlström, G.; Linse, P.; Wallquist, A.; Jönsson, B. *J. Am. Chem. Soc.* **1983**, *105*, 3777.

(26) Valteau, J. P.; Wittington, S. G.; Valteau, J. P.; Torrie, G. M. In "Modern Theoretical Chemistry"; Berne, B. J., Ed.; Plenum: New York, 1977; Vol. 5.

(27) Pangali, C.; Rao, M.; Berne, B. *J. Mol. Phys.* **1980**, *40*, 661.

(28) Matsuoka, O.; Clementi, E.; Yoshimine, M. *J. Chem. Phys.* **1976**, *64*, 1351.

(29) Wood, W. W. In "Physics of Simple Liquids"; Temperley, H. N. V., Rowlinson, J. S., Rushbrooke, G. S., Eds.; North-Holland: Amsterdam, 1968; Chapter 5.

(30) Wood, W. W. In "Fundamental Problems in Statistical Mechanics III"; Cohen, E. G. D., Ed.; North-Holland: Amsterdam, 1975.

(31) Metropolis, N. A.; Rosenbluth, A. W.; Rosenbluth, M. N.; Teller, A.; Teller, E. *J. Chem. Phys.* **1953**, *21*, 1087.

(32) Owicki, J. C.; Scheraga, H. A. *Chem. Phys. Lett.* **1977**, *47*, 600.

(33) Bigot, B.; Jorgensen, W. L. *J. Chem. Phys.* **1981**, *74*, 1944.

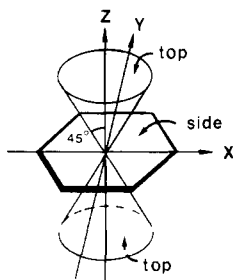


Figure 2. Orientation of the benzene molecule in the coordinate frame is shown as well as the top and side regions.

within a sphere by a hard boundary, while the hydrogens were allowed to be outside the spherical boundary. In simulation 1b, the benzene molecule was kept fixed with its center of mass at the center of the sphere. These two boundary conditions and others have previously been investigated,^{14,26,34} but it is still unclear which should be preferred in calculations of dilute solutions.

The main error in assuming pairwise additive potentials arises from the induction energy term. The benzene-water potential described will probably give a too attractive induction interaction, since each of the surrounding water molecules interacts with a benzene molecule that only experience the electric field from the interacting water molecule, and it is likely that the true field acting on a benzene molecule in a water solution will be smaller than the field from all water molecules due to cancellation effects. Thus, a better approximation would be to sum up the electric field from the water molecules at the benzene and together with the polarizability of the benzene molecule obtain the induction energy. In order to estimate the significance of the induction term in the benzene-water potential, we have performed a simulation, 2b', where the induction term was omitted.²⁵ Simulation 2b, where the induction term probably is overestimated, will then give a lower limit, and simulation 2b', where the induction term is neglected, will give an upper limit of the benzene-water energy.

The influence of benzene on the water structure was expected to be most significant for water molecules in the first hydration shell. Therefore, many quantities investigated were restricted to this shell. Simulations of smaller systems showed that the first minimum of the radial distribution function between the center of benzene and the water atoms has only a weak angular dependence. The maximum radial distance where water molecules were considered to belong to the first hydration shell was 5.89 Å, and quantities averaged over or with at least one water molecule in the shell will be denoted by an asterisk. In simulation 1w, the restriction was applied to water molecules within 5.89 Å from the center of the sphere, and in simulation 2w, all the water molecules were considered. The space around the benzene molecule was further divided into two regions, *top* and *side*. Top corresponds to the conical volumes along the symmetry axis of benzene, and side corresponds to the rest (see Figure 2).

All five simulations were performed with 200 water molecules, and averages were calculated over 2.0 million configurations except simulation 1w. Experimental density of water at 298 K was used, and the partial molar volume of benzene in water was 138.16 Å³/molecule, as given by Masterton.³⁵ Cluster radii and box dimensions are shown in Table 11. The cluster radii were 0.4-Å shorter than what was given by the water density and by the partial molar volume of benzene in water. This somewhat arbitrary choice was made in order to partially compensate for the hydrogen atoms, which were allowed to be outside the sphere. The same spherical condition, but without any compensation, has been used by Bolis et al.⁸ in their simulation of methanol in water. With periodic boundary conditions, the box length in the *z* direction was slightly shorter than that in the *x* and *y* directions in order to get the same amount of water between the benzene molecule and the box sides along the three coordinate axes.

(34) Neumann, M.; Steinhauser, O. *Mol. Phys.* **1980**, *39*, 437.
 (35) Masterton, W. L. *J. Chem. Phys.* **1954**, *22*, 1830.

Table III. Calculated Internal Energies for the Aqueous Solution of Benzene, kJ/mol^a

	simulation		
	1b	2b	2b'
U_{SW}	-6488 ± 10	-7577 ± 9	-7602 ± 11
U_W	-6513 ± 12 ^b	-7484 ± 10 ^c	-7484 ± 10 ^c
$U_{W'}$	-6424 ± 10	-7508 ± 9	-7545 ± 11
\bar{U}_S'	-63.6 ± 0.9	-68.7 ± 0.6	-56.3 ± 0.9
\bar{U}_{rel}	89 ± 16	-24 ± 14	-61 ± 16
\bar{U}_S	25 ± 16	-93 ± 14	-117 ± 17
n^*d	23.5	25.5	25.8
U_{W^*}	-71.4 ^b	-74.8 ^c	-74.8 ^c
$U_{W'^*}$	-69.2	-76.1	-77.2
$\bar{U}_{S'^*}$	-52.6	-35.8	-29.9

^aThe numbers are given with one standard deviation calculated according to ref 29 over segments of 100 000 steps. Approximately the same standard deviations were obtained by doubling the length of the segments. The standard deviations of \bar{U}_{rel} and \bar{U}_S are the square root of the sum of the component variances. ^bSimulation 1w. ^cSimulation 2w. ^dAverage number of water molecules within 5.89 Å.

The assumption of pairwise additivity implies for the total potential energy

$$U_{SW} = \bar{U}_S' + U_{W'} = \sum_{i=1}^N U_{SW_i'} + \sum_{i=1}^N \sum_{j>i}^N \epsilon_{ij}' \quad (2)$$

where \bar{U}_S' is the direct benzene-water potential energy (the bar indicates a partial molar quantity), $U_{W'}$ is the total potential energy of *N* water molecules as a solvent, U_{SW_i}' is the potential energy between the benzene molecule and one water molecule, while ϵ_{ij}' is the potential energy between two water molecules. The partial molar energy of benzene, \bar{U}_S , and the change of the internal energy of solvent induced by the solute, \bar{U}_{rel} , are defined by

$$\bar{U}_S = U_{SW} - U_W \quad (3)$$

$$\bar{U}_{rel} = U_{W'} - U_W \quad (4)$$

where U_W is the total potential energy of an equal number of water molecules as a pure liquid.

The structural arrangement of water is discussed in terms of radial distribution functions and number of hydrogen bonds. The radial distribution function between a site at benzene and a site at water will be denoted by $g_{xy}(r)$, where *x* can be a C or H atom or the center of mass (B) and *y* is either a O or H atom. Radial distribution functions between water oxygens will be referred to as $g_{OO}(r)$.

Two water molecules were considered to be hydrogen bonded if their pair potential energy, ϵ_{ij} , was lower than the threshold value ϵ_{HB} . The term $\nu(n)$ will symbolize the fraction of water molecules with *n* hydrogen bonds. Threshold values considered were -10.0, -12.0, -14.0, and -16.0 kJ/mol.

Results and Discussion

A. Benzene-Water Interaction. The partial molar energy of benzene in water may be divided into two parts. By combining eq 2, 3, and 4 we obtain

$$\bar{U}_S = \bar{U}_S' + \bar{U}_{rel} \quad (5)$$

The first term on the rhs is the interaction energy between the benzene and all water molecules, and the second term, the relaxation term, corresponds to the difference in energy between an equal number of water molecules in the solution and in pure water.

Energy data from the simulations are shown in Table III. The large standard deviations of \bar{U}_{rel} and \bar{U}_S are due to the fact that we are interested in small differences of large numbers. The observed molar enthalpy of transfer of benzene from the ideal dilute solution in water to the ideal vapor state at 303 K is 29.9 ± 0.1 kJ/mol³⁶ and the corresponding heat capacity at constant

(36) Tucker, E. E.; Land, E. H.; Christian, S. D. *J. Solution Chem.* **1981**, *10*, 21.

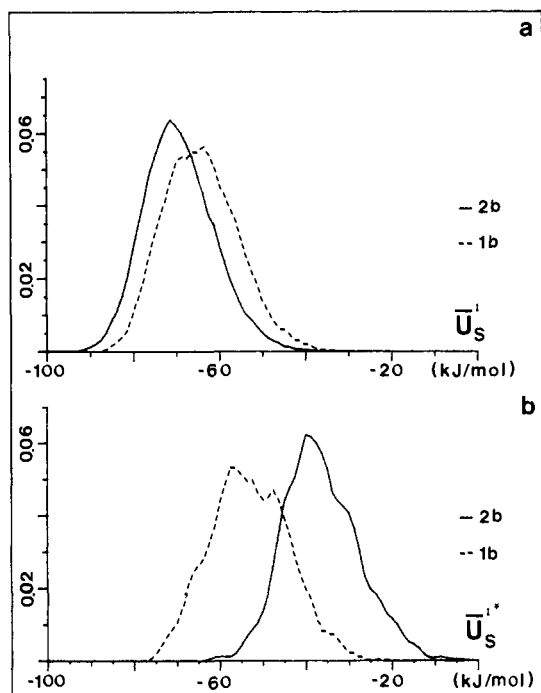


Figure 3. Distribution function of the total benzene-water interaction energy, \bar{U}_S' (a), and the distribution function of the benzene-water interaction energy constrained to water molecules in the first hydration shell, $\bar{U}_S'^*$ (b).

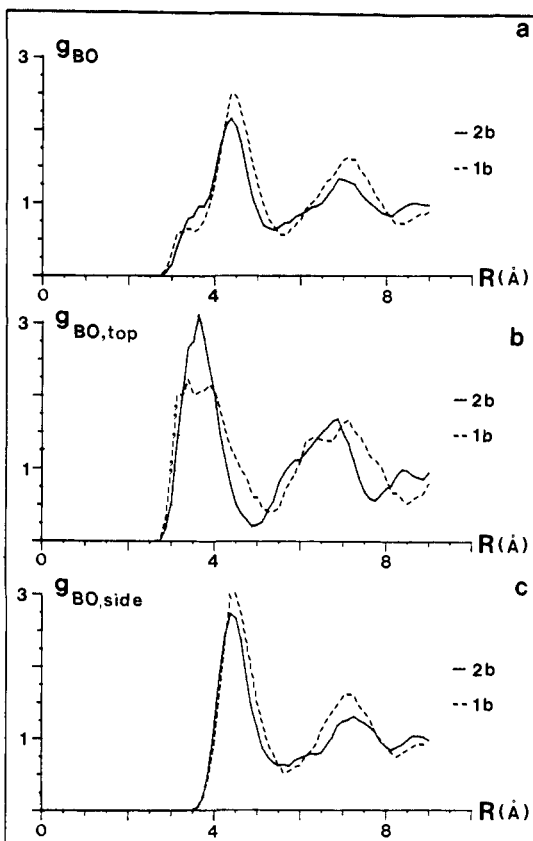


Figure 4. Radial distribution function g_{BO} . In 4a, all water molecules were considered, while in 4b, only water molecules in the top region, and in 4c, only those in the side region. The top and side regions are defined in the calculation section.

pressure -315 J/mol K. This corresponds to an experimental partial molar energy of benzene in water of -34.0 kJ/mol, a value which differs significantly from both 25 ± 16 kJ/mol obtained from the cluster model and -93 ± 14 kJ/mol from the periodic

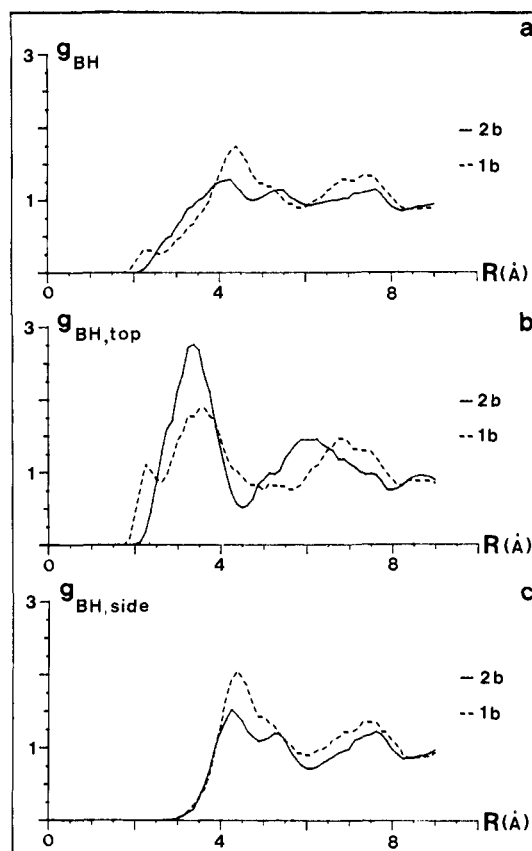


Figure 5. Same as Figure 4 but with g_{BH} .

boundary conditions. The fact that simulations only qualitatively predict partial molar energies may be due both to boundary conditions and to the intermolecular potentials. A closer investigation of the two boundary conditions used here is reported in the following section. Table III also gives the interaction energy between the benzene and water molecules in the first hydration shell, $\bar{U}_S'^*$, to -52.6 (1b) and -35.8 (2b) kJ/mol, respectively. Thus, the contribution from this shell to \bar{U}_S' is 80% and 50%, respectively, which is a large difference between the two models. The probability distribution functions of \bar{U}_S' and of $\bar{U}_S'^*$ are shown in Figure 3. The distribution functions for the two models show roughly the same dispersion, although their mean values are shifted. Table III shows that the omission of the induction term in the benzene-water potential changes \bar{U}_S' and $\bar{U}_S'^*$ by 13 and 6 kJ/mol, respectively. Thus, the induction energy may give a significant contribution to the total benzene-water interaction energy.

It is worth mentioning that the total interaction energy between benzene and water molecules is substantial, considering that benzene is a nonpolar compound. In this aspect, benzene falls somewhere between methanol,⁸ ethanol,⁹ or formaldehyde¹⁰ with calculated total interaction energies of -101 , -78 , and -92 kJ/mol and methane⁵ or argon⁷ with interaction energies of 7 and 9 kJ/mol, although the accuracy of each number has to be considered with care.

B. Benzene-Water Radial Distribution Functions. Figures 4 and 5 show the calculated g_{BO} and g_{BH} for simulations 1b and 2b. These distribution functions have been divided into two regions, top and side. This division was based on the coordinate of the oxygen atom. The first maximum of $g_{BO,top}$ and $g_{BO,side}$ is found at ~ 3.6 and 4.5 Å, which coincides with the minima of the benzene-water potential (see Figure 1). A comparison between $g_{BO,top}$ and $g_{BH,top}$ indicates that hydrogen atoms are, on the average, closer to the benzene molecule than what the oxygen atoms are, which is consistent with the pair potential (see Figure 1a). The $g_{BH,side}$ is not as structured as $g_{BH,top}$, and the first maximum of $g_{BH,side}$ is rather broad, indicating a substantial degree of orientational freedom.

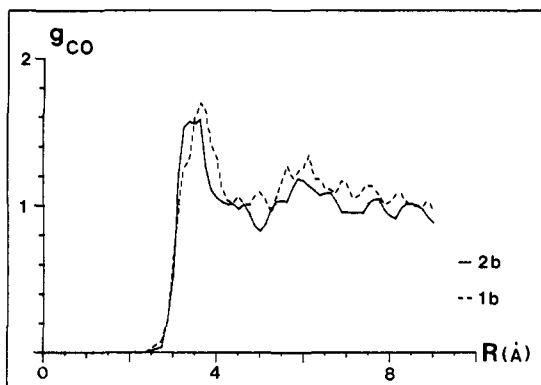


Figure 6. Atom-atom radial distribution function g_{CO} .

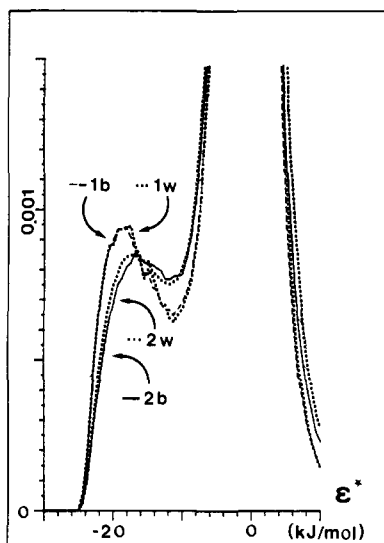


Figure 7. Probability distribution function for water-water pair energies, ϵ^* .

The total radial distribution functions, g_{BO} and g_{BH} , are weighted sums of corresponding "top" and "side" quantities. The superposition of the first maxima of $g_{BO, \text{top}}$ and $g_{BO, \text{side}}$, together corresponding to about 23 water molecules, gives one peak with a shoulder at shorter distances. The reasons are that the two maxima have different positions and that the volume of the top region is slightly less than half the volume of the side region. The calculated g_{BO} curves also show that a second hydration shell is well established with a maximum at a distance of about 7 Å, independent of the region studied. This second shell contains about 50 water molecules. On the other hand, Figure 5a shows that the radial distribution of hydrogens is much more averaged out. The small peak at 2.3 Å in simulation 1b is probably due to a water molecule located in the global minimum with one hydrogen atom pointing toward the benzene during a large number of configurations. This may seem surprising, considering the rather weak interaction, but this finding is supported by additional simulations not reported here.

We also calculated the four different atom-atom radial distribution functions. Out of these, only g_{CO} and g_{HO} exhibit any significant structure. A first coordination shell of oxygen around the carbon atoms can be seen in Figure 6. The coordination of oxygen around the benzene hydrogens is even less pronounced.

In summary, irrespective of the model, we find that the hydration of benzene is characterized by at least one, perhaps two, developed hydration shell. The average orientation of water molecules in the first shell differs between the top and the side regions. The atom-atom correlation is weak, the largest correlation being shown between carbon and oxygen.

C. Water-Water Interaction. Figure 7 shows the probability distribution function for pair energies between two water molecules, ϵ^* , where at least one is in the first hydration shell (except

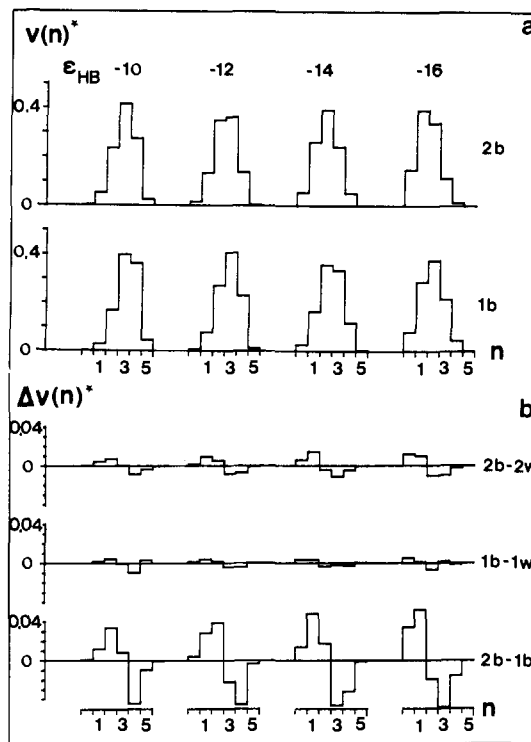


Figure 8. Probability distribution function for water molecules with n hydrogen bonds, $\nu(n)^*$, at four different threshold energies (a) and $\Delta\nu(n)^*$ (b), the difference of $\nu(n)^*$ between simulation with solvated benzene and pure water.

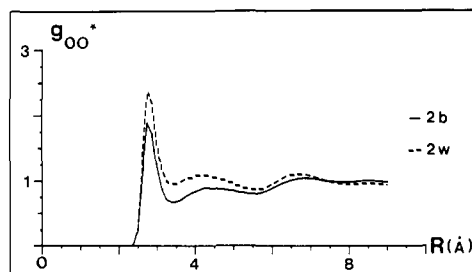


Figure 9. Radial distribution function g_{OO^*} .

simulation 2w, where all pairs were included). In the cluster model, there is no significant difference between pure water and a benzene solution. With periodic boundary conditions, there is a small decrease of strong hydrogen bonds upon solvating benzene (see also Figure 8). However, Figure 7 reveals that the largest difference is between the two models, irrespective of the presence of a benzene molecule. It seems as if the cluster model favors the formation of strong hydrogen bonds compared to periodic boundary conditions.

The analysis of the number of hydrogen bonds formed by water molecules was also restricted in the same way as ϵ^* . Figure 8 shows the probability of different numbers of hydrogen bonds, $\nu(n)^*$, for different values of the threshold energy, ϵ_{HB} , and the difference of $\nu(n)^*$. Figure 8 confirms what could already be anticipated from Figure 7, namely, that the introduction of a benzene molecule into water hardly affects the interaction between the water molecules themselves. The big difference is again found between the two types of boundary conditions. This can also be seen in Table III, where the water-water energy in the first shell, U_W^* , is different between the two models.

D. Water-Water Radial Distribution Functions. The water-water structure has been examined by the oxygen-oxygen, oxygen-hydrogen, and hydrogen-hydrogen radial distribution functions, i.e., g_{OO^*} , g_{OH^*} , g_{OH^*} . Figure 9 shows the g_{OO^*} for the simulations with periodical boundary conditions which confirms that there are no major differences between the water structure around a benzene molecule and pure water, except for a somewhat

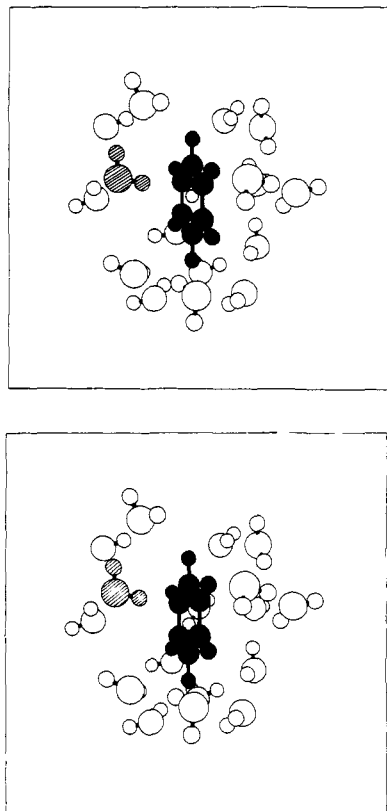


Figure 10. A stereographic view showing a benzene molecule with its nearest water neighbors.

lower amplitude at shorter distances. This is due to the benzene molecule which reduces g_{OO}^* by excluding about four water molecules but does not otherwise seem to disturb the water structure. The same conclusions can be drawn from the cluster simulations.

As a conclusion to the discussion of the water structure close to a benzene molecule, a stereographic view is presented in Figure 10 showing a typical configuration of the benzene molecule and the water molecules within 5.0 Å from the origin. The shadowed water molecule is 3.3 Å from the center of the benzene, and its orientation is close to the global energy minimum of the benzene-water potential.

Boundary Conditions

There are a number of different boundary conditions for simulation of large molecular systems. However, two types may be distinguished, one mimicking an infinite system and the other treating only a smaller part on a molecular level. The "infinite" system is usually built up of an infinite array of identical boxes in all dimensions. The energy evaluation may cover all interactions, i.e., an Ewald-type summation, or perhaps be truncated in different ways.²⁶ In our case, we have chosen a cubic cutoff, which implies that the molecule i interacts with all other molecules j that are within a fictitious box centered at i having the same dimensions as the simulation box. However, with these boundary conditions, water molecules located on opposite sides of the solute may interact in an unphysical way. Figure 11 shows the interaction between water molecules 1 and 2 in a large central box, while in a smaller system, molecule 1 will interact with the *image* of the other water molecule, 2'. How this will affect the energetics and structure of the system is difficult to predict. But this artifact is likely to be more serious in a system where an odd multipole is solvated by even multipoles or vice versa than in a system with either odd or even multipoles. Thus, benzene (quadrupole) in water (dipole) is a system where we might expect this boundary artifact to appear. It can be noted here that switching the orientation of a water molecule at the edge of the box changes the interaction energy by up to 1 kJ/mol. This difficulty may partially be overcome by using a spherical cutoff radius smaller than the box edge length.

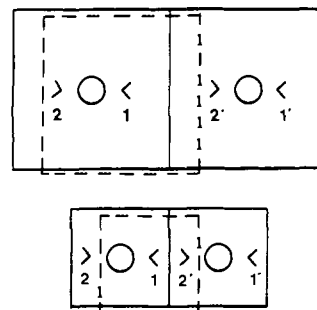


Figure 11. Upper part shows how two solvent molecules 1 and 2 close to the solute will interact with each other in a large box. However, with a large solute and/or with a small box, molecule 1 will interact with the image of the other one, 2'. The dashed line shows the fictitious box centered at molecule 1.

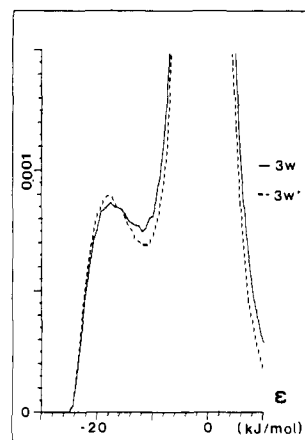


Figure 12. Probability distribution function for water-water pair energies, ϵ . The full line is obtained with normal density, $3w$, and the dashed line corresponds to 10% lower density, $3w'$. The curves are rescaled from 125 to 200 water molecules. The curve for $2w$ given in Figure 7 coincides with the one for $3w$.

The idea behind the cluster model is to describe only a part of the system on a molecular level, while the long-range interactions are either neglected or treated within a continuum theory.³⁴ In this work, the cluster is delimited by a spherical hard boundary for the oxygen atoms while the hydrogens are allowed to fall outside the boundary. This makes it difficult to define the water density in the sphere, and the orientation of the water molecules close to the boundary will also be affected. In our case, the local oxygen density was increased by 35%, and the hydrogen density was decreased by 10% in the neighborhood of the boundary (1.0-Å-thick shell).

The observed partial molar energy of benzene in water, -34.0 ± 0.1 kJ/mol,³⁶ differs significantly both from 25 ± 16 kJ/mol obtained in the cluster model and -93 ± 14 kJ/mol from the simulations with periodic boundary conditions. The difference in solvation energy seems even stranger when one notices that the direct benzene-water interaction is quite similar, -64 and -69 kJ/mol for simulations 1b and 2b, respectively. Almost the entire difference may thus be assigned to the water relaxation energy which is repulsive with 89 ± 16 kJ/mol and attractive with -24 ± 14 kJ/mol, respectively (see Table III), giving a difference in the relaxation energy between the two models of 113 ± 21 kJ/mol.

Table III shows that the number of water molecules in the first hydrogen shell, n^* , is about 9% lower in the cluster model than with periodic boundary conditions. In order to better understand this result as well as other differences between the two models (Figures 7 and 8), we have investigated the effect of a lower density. Two additional simulations on pure water with 125 water molecules were performed, one with the same conditions as $2w$, called $2w'$, and one with 10% lower density, $3w'$. Figure 12 shows the distribution function of the water-water pair energy, and Figure 13 shows the difference of the number of hydrogen bonds.

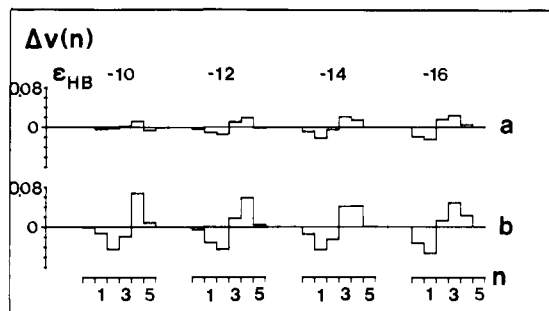


Figure 13. Probability distribution function $\Delta v(n)$ for different pure water simulations: (a) $\nu(n)_{3w} - \nu(n)_{3w}$; (b) $\nu(n)_{1w^*} - \nu(n)_{3w}$.

Figure 13 and a comparison between Figures 7 and 12 indicate that a 10% decrease in the density may explain half the difference in the water-water interaction between simulations 1b and 2b. Thus, the effect from different water density, if any, is not sufficient to explain the differences in Figures 7 and 8 between the cluster model and simulations with periodical boundary conditions.

The cluster model suffers from the truncation of all interactions at the sphere boundary. However, this can be at least partly compensated for by solvating the cluster in a dielectric continuum. The difference in solvation energy for the water cluster and the water + benzene cluster may be divided into two parts: one arising from the difference in cluster radii and a second one due to the presence of the benzene molecule. The solvation energy for a pure water cluster with a radius R is given by

$$U^S(R) = \gamma \cdot A \quad (6)$$

and for a cluster with radius R and ΔR

$$U^S(R + \Delta R) = \gamma' A' = (\gamma + \Delta\gamma)(A + \Delta A) \approx \gamma A + \gamma \Delta A + \Delta\gamma A \quad (7)$$

where we have omitted the term quadratic in Δ . The term A in eq 6 and 7 is the area of the cluster and γ the surface internal energy, which for H_2O is somewhat larger (0.118 J/m^2) than the surface free energy (0.072 J/m^2) at room temperature.³⁷ Thus, the second term on the rhs of eq 7 will give a 19.1 kJ/mol more exothermic solvation energy when changing the radius from 10.86 to 10.96 Å. It is, however, considerably more difficult to estimate the change in the surface tension due to the change in radius.³⁸⁻⁴⁰

(37) Davies, J. T.; Rideal, E. K. "Interfacial Phenomena"; Academic Press: New York and London, 1963.

Following the ideas of Benson and Shuttleworth,⁴⁰ one may estimate this contribution to be $<1 \text{ kJ/mol}$. The other part, which may be viewed as the difference in relaxation energy between the cluster model and an infinite system, can be estimated in a continuum approximation, and it is found to be negligible ($\leq 1 \text{ kJ/mol}$). Thus, we find that neither a change in the water density nor simple continuum corrections in the cluster model are able to explain the discrepancy between the different solvation energies found in this model and the model with periodic boundary conditions.

The dependence on the structure in pure water of boundary conditions has earlier been investigated by Pangali et al.²⁷ In a comparison between a cubic and a spherical cutoff with periodic boundary conditions, they found that the number of hydrogen bonds was larger in the latter case. They also found that the structure was heavily dependent on the cutoff distance. Thus, from their and our studies, it seems crucial to use the same boundary conditions when making comparative investigations, although still effects from the boundary conditions may not be negligible.

Conclusions

The benzene-water pair potential shows a rather strong orientation dependence mainly due to the dipole-quadrupole interaction. This preferential orientation is also reflected in the orientation of water molecules in the first hydration shell of benzene. The water structure is only slightly perturbed by the presence of the benzene molecule, although both a first and a second hydration shell are discernable.

However, the main observation from our simulations is that different boundary conditions may lead to quite different results. This is certainly true for global properties like the solvation energy and maybe to a lesser extent for more local properties like the benzene-water distribution functions, confined to the first hydration shell. Neither of the two models considered is able to reproduce experimental results for the solvation energy, and there does not seem to be any obvious choice of model. Further methodological studies are certainly warranted.

Acknowledgment. P.L. acknowledges a grant from Stiftelsen Bengt Lundquists Minne.

Registry No. Water, 7732-18-5; benzene, 71-43-2.

(38) Tolman, R. C. *J. Chem. Phys.* **1949**, *17*, 333.

(39) Kirkwood, J. G.; Buff, F. P. *J. Chem. Phys.* **1949**, *17*, 338.

(40) Benson, G. C.; Shuttleworth, R. *J. Chem. Phys.* **1951**, *19*, 130.

Aqueous Hydration of Benzene

G. Ravishanker, P. K. Mehrotra, M. Mezei, and D. L. Beveridge*

Contribution from the Hunter College of the City University of New York, New York, New York 10021. Received October 12, 1983

Abstract: A (T, V, N) ensemble Monte Carlo computer simulation has been performed on a dilute aqueous solution of benzene at 25 °C. The calculation employs intermolecular pairwise potential functions determined from quantum mechanical calculations. The results are analyzed by means of the proximity criterion, which permits the hydration to be described on a solute atom or molecular fragment basis. The results indicate the first solvation shell hydration complex of benzene consists of some 23 water molecules. The in-plane hydration is found to be essentially hydrophobic. The π -cloud hydration involves a first shell of two water molecules situated one above and one below the molecular plane, and the nature of interaction has both hydrophilic and steric attributes. Results are discussed in comparison with recent simulation studies of alkyl groups.

In view of the importance of the hydrophobic effect in structural biochemistry, a knowledge of the details of the hydrophobic hydration of prototype apolar species at the molecular level is quite

desirable. Recent research studies from this laboratory have employed liquid-state computer simulations to study the structure and energetics of dilute aqueous solutions of CH_4 ,¹ a prototype